J. Membrane Biol. 91, 275–284 (1986)

The Journal of
Membrane Biology

Microscopic Description of Voltage Effects on Ion-Driven Cotransport Systems

P. Läuger and P. Jauch
Department of Biology, University of Konstanz, D-7750 Konstanz, Federal Republic of Germany

Summary. A microscopic model for the analysis of voltage effects on ion-driven cotransport systems is described. The model is based on the notion that the voltage dependence of a given rate constant is directly related to the amount of charge which is translocated in the corresponding reaction step. Charge translocation may result from the movement of an ion along the transport pathway, from the displacement of charged ligand groups of the ion-binding site, or from reorientation of polar residues of the protein in the course of a conformational transition. The voltage dependence of overall transport rate is described by a set of dimensionless coefficients reflecting the dielectric distances over which charge is displaced in the elementary reaction steps. The dielectric coefficients may be evaluated from the shape of the experimental flux-voltage curve if sufficient information on the rate constants of the reaction cycle is available. Examples of flux-voltage curves which are obtained by numerical simulation of the transport model are given for a number of limiting cases.

Key Words cotransport systems · electrogenic transport · voltage dependence · charge movement · current-voltage characteristic

Introduction

Cotransport systems that utilize an electrochemical gradient of H^+ or Na^+ as a driving force for the accumulation of substrates are widespread in cellular membranes. Well-studied examples are the sodium-coupled glucose cotransporter of small intestine (Crane & Dorando, 1982; Semenza et al., 1984; Stevens, Kaunitz & Wright, 1984), the sodium-coupled amino acid transport systems of animal cells (Johnstone, 1979; Stevens et al., 1984), and the H^+/galactoside cotransport system of *Escherichia coli* (Kaback, 1983; Overath & Wright, 1983).

Most cotransport systems studied so far are electrogenic, i.e., they transport net electric charge across the membrane. This leads to a number of interesting phenomena. The cotransport system may interact with and may be controlled by the electric field in the membrane; furthermore, the cotransporter contributes to the electric conductance of the membrane. An important experimental aspect is the possibility of obtaining information on the transport mechanism by studying the voltage dependence of transport rates (Kessler & Semenza, 1983; Aronson, 1984; Restrepo & Kimmich, 1985*a*, 1986).

In this paper we describe a microscopic model for the analysis of voltage effects on ion-driven cotransport systems. The model is based on the notion that the voltage dependence of a given rate constant is directly related to the amount of charge that is translocated in the corresponding reaction step. Charge translocation may result from the movement of an ion along the transport pathway in the protein, from the displacement of charged ligand groups of the ion-binding site, or from reorientation of polar residues of the protein in the course of a conformational transition. From the experimentally observed voltage-dependence of transport rates, inferences can be made on the magnitude of charge translocation associated with the single reaction steps.

Description of the Transport Model

The analysis given below is based on the reaction scheme of Fig. 1 in which it is assumed that the cotransporter C forms a ternary complex MCS with the driving ion M^+ and the substrate S (Schultz & Curran, 1970; Turner, 1983; Sanders, Hansen, Gradmann & Slayman, 1984; Harrison, Rowe, Lumsden & Silverman, 1984; Restrepo & Kimmich, 1985*b*). The binding sites for M^+ and S are accessible either from the cytoplasmic side (states C', MC', $C'S$, $MC'S$) or from the extracellular side (states C'', MC'', $C''S$, $MC''S$). It is further assumed that conformational transitions switching the binding site from the inward-facing to the outward-fac-

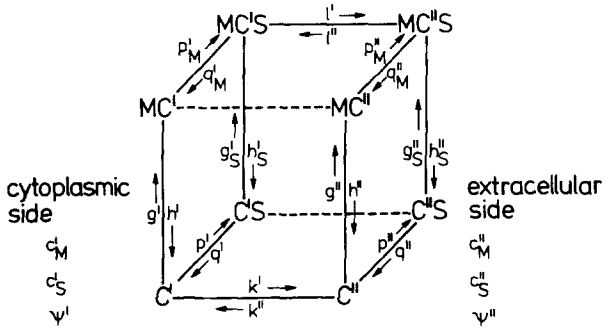

Fig. 1. Transport of ion M^+ and substrate S by a cotransporter C. The binding sites for M^+ and S are accessible either from the cytoplasmic side (states C', MC', $C'S$, $MC'S$) or from the extracellular side (states C'', MC'', $C''S$, $MC''S$). It is assumed that conformational transitions switching the binding sites from the inward-facing to the outward-facing configuration are possible only in the empty and the fully occupied states (C and MCS). k', k'', g', h', etc., are rate constants. c'_M, c'_S and ψ' are the concentrations of M^+ and S and the electric potential at the cytoplasmic side; c''_M, c''_S and ψ'' refer to the extracellular side

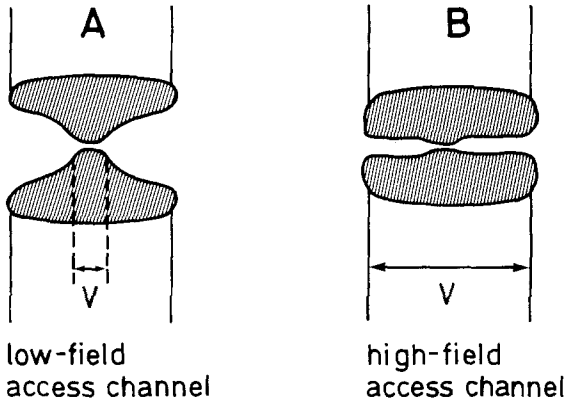

Fig. 2. Two limiting cases for the structure of the access channel connecting the binding sites with the aqueous medium. (*A*) Access channel consisting of a wide, water-filled pore (or vestibule) with a high electrical conductance; the electric field strength in the access channel is low so that a large fraction of the transmembrane voltage V drops across the narrow, "gating" part of the molecule. (*B*) Narrow and specific access channel, allowing the entry of the driving ion but not of other ion species; in this case the electric-field strength in the access channel is high, so that the rate constants for ion binding and release become voltage dependent ("ion-well" behavior)

ing configuration are possible only in the empty ($C' \rightleftarrows C''$) and in the fully-occupied state ($MC'S \rightleftarrows MC''S$). The reaction scheme depicted in Fig. 1 is specifically based on a 1 M^+ : 1 S stoichiometry, but the treatment can be extended easily to other stoichiometries.

The kinetic properties of the transport model are described by the rate constants k', k'', g', h', etc. (Fig. 1); h', k', l', and q' are monomolecular rate constants (expressed in sec^{-1}), whereas g' and p' refer to bimolecular association reactions and are expressed in M^{-1} sec^{-1}. According to the principle of microscopic reversibility, the rate constants are connected by the following relations:

$$p'g'_S q'_M h' = q'g'p'_M h'_S \tag{1}$$

$$p''g''_S q''_M h'' = q''g''p''_M h''_S \tag{2}$$

$$g'p'_M l'q''_M h''k'' = g''p''_M l''q'_M h'k' \cdot \exp(u) \tag{3}$$

$$u \equiv \frac{\psi' - \psi''}{kT/e_0} = \frac{V}{kT/e_0} \tag{4}$$

ψ' and ψ'' are the electric potentials in the cytoplasm and the extracellular medium, respectively, and u is the transmembrane voltage, expressed in units of $kT/e_o \simeq 25$ mV (k, Boltzmann constant; T, absolute temperature; e_o, elementary charge). Equations (1)–(3) state that for any cycle of the reaction scheme of Fig. 1 the products of the rate constants in clockwise and in counterclockwise direction must be equal at $u = 0$; the factor $\exp(u)$ accounts for the fact that charge is transferred across the membrane when the system goes through the cycle

$C' \rightarrow MC' \rightarrow MC'S \rightarrow MC''S \rightarrow MC'' \rightarrow C'' \rightarrow C'$.

For the derivation of Eqs. (1)–(3), *see* Läuger (1984).

Voltage Dependence of Rate Constants

The current-voltage behavior of the cotransport system is determined by the voltage dependence of the individual transport steps. It is often assumed that only a single step, the transition between states with inward-facing and outward-facing binding sites, is affected by voltage (Geck & Heinz, 1976; Turner, 1981; Sanders et al., 1984). This assumption, if taken literally, would mean that the ion binding site has to move over the whole dielectric distance over which the transmembrane voltage drops. Such a large-scale movement is unlikely, however, in the case of a transport protein spanning the entire lipid bilayer (Semenza et al., 1984).

A possibility to overcome this difficulty consists in the assumption that the binding site is connected with the aqueous medium by an access channel. The distance over which the binding site moves in the conformational transition may then be much smaller than the membrane thickness. Two limiting cases for the geometry of the access channel are feasible. The access channel may be a wide, water-filled pore with a low electric resistance (Fig. 2*A*); in this case the electric field strength in the access

channel is small so that a large fraction of the voltage drops across the narrow gating part of the molecule. Alternately, the access channel may be narrow and specific, allowing entry of the driving ion but not of other ion species (Fig. 2*B*). The access channel then behaves as an "ion well" (Mitchell 1969; Hopfer & Groseclose, 1980; Aronson, 1984; Restrepo & Kimmich, 1985*a*), i.e., part of the transmembrane voltage drops between binding site and external medium, so that the rate constants for ion binding and release become voltage dependent.

In order to describe the voltage dependence of the rate constants, we introduce the energy profile of the driving ion M^+ along the transport pathway, which consists of a series of barriers and wells (Fig. 3). In conformation C' the ion binding site is connected with the cytoplasmic side by a series of low barriers, but separated from the extracellular side by a barrier of virtually infinite height. In conformation C'' the barrier toward the cytoplasm is high and the barrier toward the extracellular medium low. A parallel pathway through the transport protein is assumed to exist for the substrate S, the binding site of S being connected with the cytoplasm in conformation C' and with the extracellular medium in conformation C''. The model of a gated channel, which is used here, has been extensively discussed in the literature (Patlak, 1957; Jardetzky, 1966; Klingenberg et al., 1976; Läuger, 1980); it has been explicitly applied to ion-driven cotransport by Kessler and Semenza (1983).

According to Fig. 3, it is assumed that the exchange of ions between binding site and cytoplasm is restricted by a rate-limiting barrier. It is further assumed that the other barriers toward the cytoplasm are low, so that an equilibrium always exists between energy well W' (Fig. 3) and the cytoplasm. In the presence of a transmembrane voltage V, a fraction $\beta' V$ of the voltage drops between the cytoplasm and W', and a fraction $\gamma' V$ across the rate-limiting barrier. The quantities β' and γ' depend on the geometrical distance of the energy minima as well as on the dielectric properties of the membrane. (For a homogeneous membrane of thickness d the relation $\beta' = b/d$ would hold, where b is the distance between W' and the cytoplasmic membrane-solution interface.) The effective ion concentration in well W' is proportional to $c'_M \exp(-\beta' e_o V/kT) = c'_M \exp(-\beta' u)$ where c'_M is the cytoplasmic ion concentration. According to the transition-state theory of reaction rates (Zwolinski, Eyring & Reese, 1949), the rate constants for binding and release of the ion at the cytoplasmic side ($M^+ + C' \rightleftarrows MC'$) are given by (Fig. 1):

$$g' = \tilde{g}' \exp[(\beta' + \gamma'/2)u] \tag{5}$$

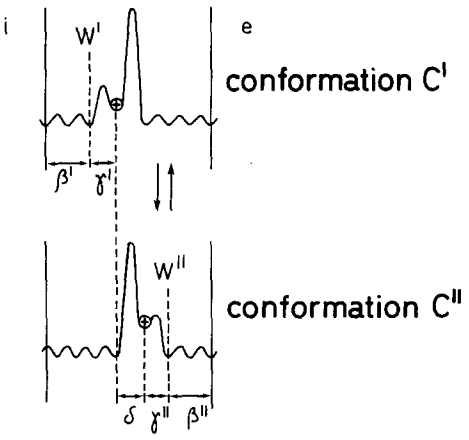

Fig. 3. Energy profile of the driving ion M^+ along the transport pathway. In conformation C' the ion-binding site is accessible from the cytoplasmic side, but separated from the external medium by a high energy barrier. In conformation C'' the binding side is accessible from the external medium. β', β'', γ', γ'' and δ are the dielectric distances along the pathway of the ion

$$h' = \tilde{h}' \exp[-\gamma' u/2]. \tag{6}$$

$\tilde{g}'$ and $\tilde{h}'$ are the values of g' and h' at zero voltage. Implicit in Eqs. (5) and (6) is the assumption that the rate-limiting barrier is narrow and symmetric so that half of the voltage drop $\gamma' u$ occurs between the top of the barrier and the adjacent wells. Analogous equations hold for the reaction $M^+ + C'S \rightleftarrows MC'S$:

$$g'_S = \tilde{g}'_S \exp[(\beta'_S + \gamma'_S/2)u] \tag{7}$$

$$h'_S = \tilde{h}'_S \exp[-\gamma'_S u/2]. \tag{8}$$

Since binding of substrate may induce a structural change of the protein, the dielectric distances β'_S and γ'_S are, in general, different from β' and γ'. It is reasonable, however, to assume that binding and release of the neutral substrate S is not affected by voltage. This means that

$$p' = \tilde{p}'; \; q' = \tilde{q}'; \; p'_M = \tilde{p}'_M; \; q'_M = \tilde{q}'_M. \tag{9}$$

Equations for the rate constants at the extracellular side (g'', h'', . . .) are obtained from Eqs. (5)–(9) by the substitutions $\beta' \rightarrow -\beta''$, $\gamma' \rightarrow -\gamma''$, $\beta'_S \rightarrow -\beta''_S$ and $\gamma'_S \rightarrow -\gamma''_S$.

In the course of the conformational transition $C' \rightarrow C''$ the ion binding site, in general, moves over a certain distance. The electrostatic contribution to the energy difference between states C' and C'' may be written as $-z_L e_o \delta V$, where $z_L e_o$ is the charge of the empty ligand system and δ is the fractional dielectric distance over which the site moves (Fig. 3). Additional charge displacements may result from

reorientation of polar residues other than the ligand groups. For instance, α-helices have a large dipolar moment corresponding to about half an elementary charge at either end of the helix (Hol, 1985). For the description of charge movements associated with a conformational transition, the protein is considered as an assembly of point charges. Motion of the i-th charge in the presence of a transmembrane voltage V results in an energy change of magnitude $-e_o\eta_i V$, where η_i is the dielectric distance over which the charge moves. The total energy change ΔU is the sum of the contributions of all individual charge displacements:

$$\Delta U = -e_o V \sum_i \eta_i = -e_o V \eta. \tag{10}$$

According to reaction-rate theory the conformational transition may be treated as a passage over an energy barrier. Assuming a narrow, symmetrical barrier, the barrier height changes by about $\Delta U/2$ in the presence of a transmembrane voltage V. This leads to the following expressions for the rate constants of the conformational transitions $C' \rightarrow C''$ and $MC'S \rightarrow MC''S$:

$$k' = \tilde{k}' \exp[(z_L\delta + \eta)u/2] \tag{11}$$

$$l' = \tilde{l}' \exp\{[(z_L + 1)\delta + \eta]u/2\}. \tag{12}$$

The rate constants for the reverse transitions (k'', l'') are obtained from Eqs. (11) and (12) by changing the sign of the exponent. According to Eqs. (1)–(3), (5)–(8), (11) and (12), the dielectric coefficients obey the following relations:

$$\beta' + \gamma' = \beta'_S + \gamma'_S \tag{13}$$

$$\beta'' + \gamma'' = \beta''_S + \gamma''_S \tag{14}$$

$$\beta' + \beta'' + \gamma' + \gamma'' + \delta = 1. \tag{15}$$

Numerical Evaluation of Transport Rates

For the numerical evaluation of transport rates we introduce the fraction $x[A_i]$ of the cotransporter present in state A_i. The eight quantities $x[A_i]$ can be obtained from the steady-state conditions $d(x[A_i])/dt = 0$. For instance, from $d(x[C'])/dt = 0$ one gets:

$$k''x[C''] + q'x[C'S] + h'x[MC'] - (k' + g'c'_M + p'c'_S)x[C'] = 0 \tag{16}$$

(*compare* Fig. 1). Since only seven of the totally eight equations of the form of Eq. (16) are independent, one of the equations is replaced by the condition that the sum of all $x[A_i]$ is unity. In this way the steady-state values of the $x[A_i]$ can be determined numerically, using the matrix inversion method (Johnson, 1980). The net (steady-state) outward fluxes of S and M^+ are then obtained from the relation

$$\Phi_S = \Phi_M = l'x[MC'S] - l''x[MC''S]. \tag{17}$$

(Note that under the assumptions of the model the fluxes of M^+ and S are completely coupled so that $\Phi_S = \Phi_M$.)

Unidirectional (isotope) fluxes may be calculated in the same way by numerical simulation of the transport system. If the substrate S is present as an isotope pair $S1$, $S2$, the unidirectional outward flux Φ'_S and the unidirectional inward flux Φ''_S are defined by

$$\Phi'_S \equiv \frac{c'_{S1} + c'_{S2}}{c'_{S1}} \Phi_{S1} \qquad (c''_{S1} = 0) \tag{18}$$

$$\Phi''_S \equiv -\frac{c''_{S1} + c''_{S2}}{c''_{S1}} \Phi_{S1} \qquad (c'_{S1} = 0). \tag{19}$$

Φ_{S1} and Φ_{S2} may be evaluated from relations analogous to Eqs. (16) and (17) after introduction of isotopic states $MC'S1$, $MC'S2$, etc.

Voltage-Dependence of Fluxes

Depending on the values of the rate constants and the dielectric coefficients, theoretically predicted flux-voltage curves may assume a variety of different shapes. In the following we consider a number of limiting cases for voltage effects on cotransport rates. In order to keep the number of free parameters as small as possible, we assume that the rate constants for binding and release of M^+ and S are much larger than the rate constants of conformational transitions so that the binding-unbinding reactions are always in equilibrium. We further assume that the transport system is symmetric (at zero voltage) with respect to the rate constants and that M^+ and S bind independently. Under these conditions all binding equilibria are described by two equilibrium constants $\tilde{K}_M$ and $\tilde{K}_S$:

$$\frac{\tilde{h}'}{\tilde{g}'} = \frac{\tilde{h}''}{\tilde{g}''} = \frac{\tilde{h}'_S}{\tilde{g}'_S} = \frac{\tilde{h}''_S}{\tilde{g}''_S} \equiv \tilde{K}_M \tag{20}$$

$$\frac{\tilde{q}'}{\tilde{p}'} = \frac{\tilde{q}''}{\tilde{p}''} = \frac{\tilde{q}'_M}{\tilde{p}'_M} = \frac{\tilde{q}''_M}{\tilde{p}''_M} \equiv \tilde{K}_S. \tag{21}$$

Furthermore, if M^+ and S bind independently, the potential profile for M^+ is the same with and without bound S; this means that

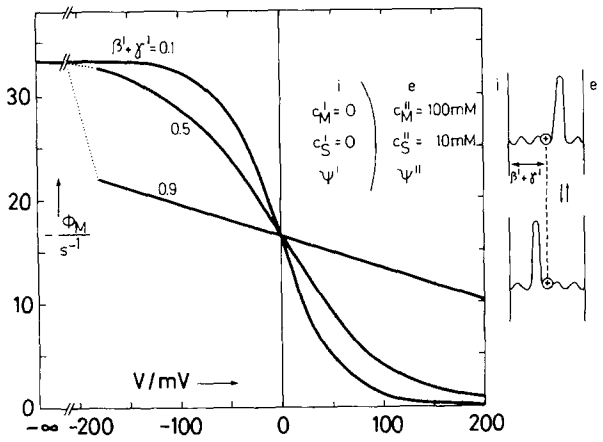

Fig. 4. Influx $-\Phi_M$ of M^+ (referred to a single cotransporter molecule) as a function of transmembrane voltage V for zero internal concentrations of M^+ and S. The following parameter values have been used for the numerical simulation: $\tilde{K}_M = 100$ mM, $\tilde{K}_S = 10$ mM, $\tilde{k}' = \tilde{k}'' = \tilde{l}' = \tilde{l}'' = 100\ \text{sec}^{-1}$, $\delta = \eta = 0$, $z_L = -1$, $c_M'' = 100$ mM, $c_S'' = 10$ mM

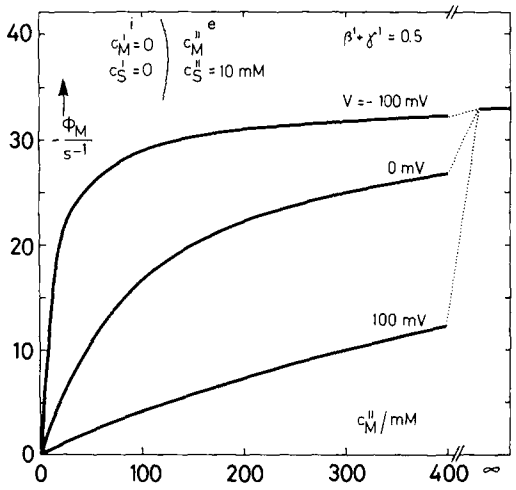

Fig. 5. Influx $-\Phi_M$ of M^+ as a function of extracellular concentrations c_M'' of M^+ for three different values of transmembrane voltage $V = \psi' - \psi''$. The experimental conditions and the values of the kinetic parameters are the same as in Fig. 4. The half-saturation concentrations are $c_M'' = 10$ mM ($V = -100$ mV), 90 mM (0 mV) and 700 mM (100 mV)

$$\beta' = \beta_S'; \beta'' = \beta_S''; \gamma' = \gamma_S'; \gamma'' = \gamma_S''. \tag{22}$$

High-Field Access-Channel; Conformational Transitions Voltage-Independent

When the access channel has a high electric resistance, a substantial fraction of transmembrane voltage drops between the ion binding site and the aqueous phase. A limiting case is given when the ion-binding site does not appreciably move in the conformational transition ($\delta \approx 0$) and when intrinsic charge displacements are small ($\eta \approx 0$). In this case the voltage dependence of Φ_S and Φ_M exclusively results from the "ion-well" effect, i.e., from the voltage dependence of the equilibrium dissociation constants $K_M' = h'/g'$ and $K_M'' = h''/g''$:

$$K_M' = \tilde{K}_M \exp[-(\beta' + \gamma')u] \tag{23}$$
$$K_M'' = \tilde{K}_M \exp[(\beta'' + \gamma'')u]. \tag{24}$$

Flux-voltage curves for three different values of $\beta' + \gamma' = 1 - (\beta'' + \gamma'')$ are represented in Fig. 4 under the condition of vanishing internal concentrations of M^+ and S. It is seen that the net influx $-\Phi_M$ ($= -\Phi_S$) saturates at negative membrane potentials V. Such a saturation always occurs when the overall transport reaction contains a voltage-independent step which at high voltages becomes rate limiting. In the example considered here the voltage-independent step is the transition between inward-facing and outward-facing configuration of the binding sites. As it is seen from Fig. 4, the shape of the flux-voltage curve strongly depends on the value of the parameter $(\beta' + \gamma')$, which reflects the location of the ion-binding site with respect to the membrane surface. When the binding site is located close to the extracellular surface ($\beta' + \gamma' = 0.9$), the voltage dependence of net inward flux is much smaller than when the site is near the cytoplasmic surface ($\beta' + \gamma' = 0.1$). This is, of course, what one would expect for an "ion-well" situation if driving ions are present only on the extracellular side. Thus, in order to obtain information on the location of the ion-binding site, it is advantageous to use asymmetric conditions ($c_M' \ll c_M''$ or $c_M' \gg c_M''$) in measuring the flux-voltage curve.

The most obvious manifestation of an ion-well situation is the voltage dependence of the relationship between flux and ion concentration. In Fig. 5 the influx $-\Phi_M$ is plotted as a function of extracellular ion concentration c_M'' for three different membrane potentials V, under the same experimental conditions as in Fig. 4. Figure 5 shows that at $V = -100$ mV (cell interior negative) the flux saturates at a much lower ion concentration than at $V = +100$ mV, the half-saturation concentrations being $c_M'' = 10$ mM ($V = -100$ mV), 90 mM (0 mV), and 700 mM (100 mV).

Low-Field Access Channel; Ion-Binding Voltage-Independent

In this section we consider the case that the access channel is a wide aqueous pore (or vestibule) with a low electric resistance (Fig. 2A). The ion-binding

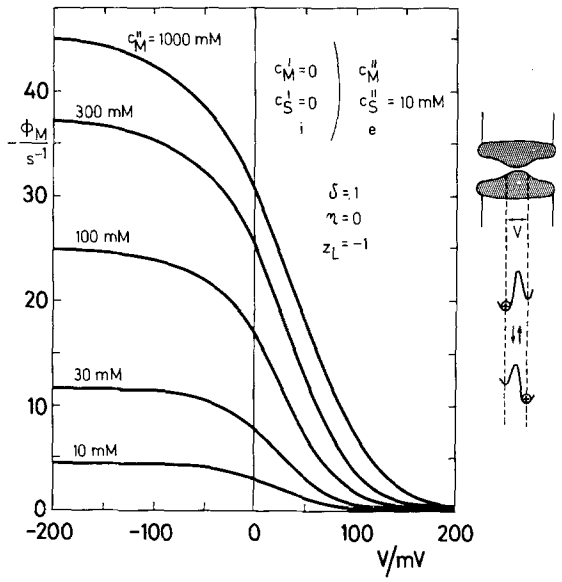

Fig. 6. Influx $-\Phi_M$ of M^+ as a function of voltage V. Low-field access channel with voltage-independent ion binding and negligible intrinsic charge displacement ($\eta = 0$); the empty ion-binding site bears a single negative charge ($z_L = -1$). $\beta' = \beta'' = \gamma' = \gamma'' = 0$, $\delta = 1$. The other kinetic parameters are the same as in Fig. 4

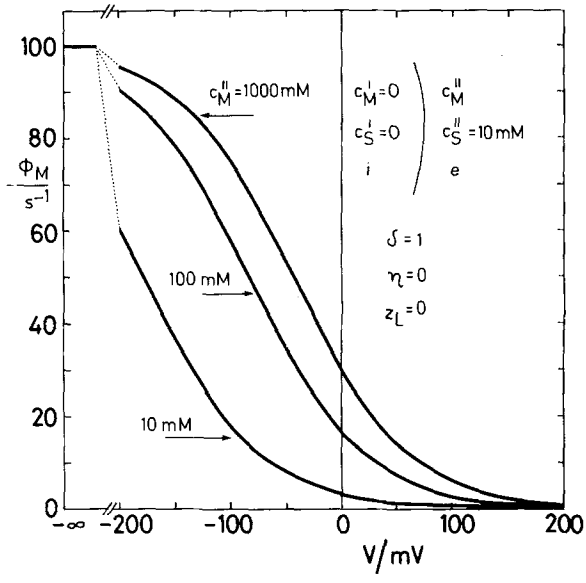

Fig. 7. Influx $-\Phi_M$ of M^+ as a function of voltage V for a cotransporter with neutral ligand system of the ion-binding site ($z_L = 0$). The other conditions are the same as in Fig. 6

site is assumed to be located in the vestibule (at the rear end) so that the rates of binding and dissociation of M^+ are not affected by voltage ($\beta' = \beta'' = \gamma' = \gamma'' = 0$; $\delta = 1$). The whole effect of membrane potential on ion and substrate fluxes then results from the voltage dependence of the conformational transitions $C' \rightleftarrows C''$ and $MC'S \rightleftarrows MC''S$.

$\eta = 0$, $z_L = -1$

Flux-voltage curves for the case that the empty ion-binding site has a single negative charge ($z_L = -1$) and that intrinsic charge displacements in the conformational transition are negligible ($\eta = 0$) are represented in Fig. 6. The inward flux $-\Phi_M (= -\Phi_S)$ at zero internal concentrations of M^+ and S saturates at negative membrane potentials V, the saturation level being dependent on the extracellular ion concentration c''_M. This behavior results from the fact that for $z_L = -1$ and $\eta = 0$ the conformational transition $MC'S \rightleftarrows MC''S$ is voltage independent and becomes rate limiting at large inward driving force. At higher concentrations of M^+ more transporter molecules are in states $MC'S/MC''S$ and therefore the saturation level of Φ_M increases with increasing c''_M.

$\eta = 0$, $z_L = 0$

When the ligand system of the ion-binding site is electrically neutral ($z_L = 0$) and when intrinsic charge displacements are negligible ($\eta = 0$), the conformational transition $C' \rightleftarrows C''$ is voltage independent and limits the flux at large inward driving force. For $c'_M = c'_S = 0$ and $V \to -\infty$ the reactions $MC''S \rightleftarrows MC'S \rightleftarrows C' + S + M^+$ are strongly poised to the right, so that virtually all transporter molecules accumulate in state C' with inward-facing binding sites, irrespective of the external concentration of M^+. The maximum flux at strongly negative membrane potentials should therefore be independent of c''_M. This expectation is borne out by the numerical analysis (Fig. 7). A comparison of Figs. 6 and 7 shows that the behavior of the transport system strongly depends on whether the ligand system is neutral or negatively charged. While in both cases the influx saturates at hyperpolarizing voltages, the saturation value of the flux increases with extracellular ion concentration c''_M for $z_L = -1$, but is insensitive to c''_M for $z_L = 0$.

$\eta \neq 0$, $z_L = -1$

When the conformational transition is associated with intrinsic charge displacements in the protein (other than movements of the ion-binding site), the parameter η in Eqs. (11) and (12) differs from zero. η is the effective number of elementary charges which are translocated across the membrane dielectric in the course of the conformational transition.

For $\eta = \frac{1}{2}$ both rate constants of conformational transitions in forward direction of the transport cycle have the same voltage dependence: $k' = \bar{k}' \exp(-u/4)$, $l'' = \bar{l}'' \exp(-u/4)$. Under this condition the inward flux increases exponentially with increasing negative membrane potentials (Fig. 8) provided that the association-dissociation reactions of M^+ and S are not rate limiting.

For $\eta < 0$ a negative charge is moved inward in the transitions with empty ($C'' \rightarrow C'$) as well as with occupied binding site ($MC''S \rightarrow MC'S$). At large negative membrane potentials a strong driving force then exists which tends to lock the transporter in states with outward-facing binding site. This leads to a decline of inward flux at hyperpolarizing voltages (Fig. 8), corresponding to a negative slope in the current-voltage characteristic of the transport system. Such a negative-resistance behavior is observed whenever the transport cycle $MC''S \rightarrow MC'S \rightarrow C' \rightarrow C'' \rightarrow MC''S$ contains steps with opposite voltage dependence. This means that a negative slope in the flux-voltage curve can occur at any charge of the ion-binding site, provided that $|\eta|$ is large enough. It is obvious that in this way the activity of a cotransport system can be regulated by a transmembrane voltage.

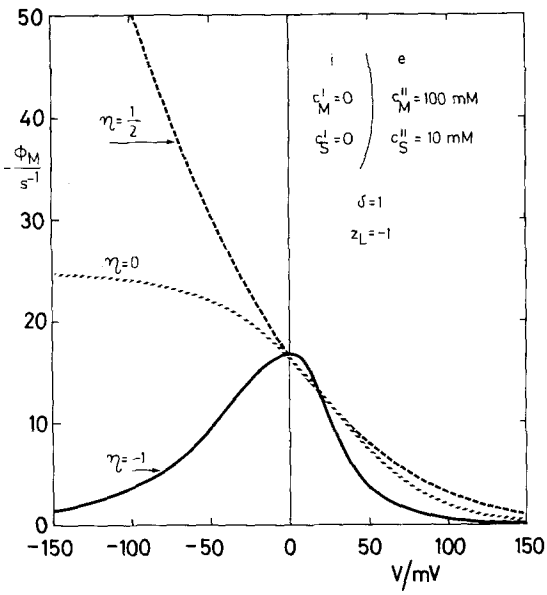

Fig. 8. Influx $-\Phi_M$ of M^+ as a function of voltage V for negatively-charged ion-binding site ($z_L = -1$) and nonzero intrinsic charge displacements ($\eta \neq 0$). The other conditions are the same as in Fig. 6. η is the effective number of elementary charges which are translocated across the membrane dielectric in the course of the conformational transition. The curve for $\eta = 0$ is reproduced from Fig. 6

Kinetics of Inhibitor Binding

In studies of Na^+-coupled D-glucose transport, phlorizin has been widely used as an inhibitor (Aronson, 1978; Turner & Silverman, 1981; Toggenburger, Kessler & Semenza, 1982; Restrepo & Kimmich, 1986). Phlorizin competes for the sugar-binding site but is not itself translocated. Measuring the rate of binding and release of the inhibitor as a function of Na^+ concentration and voltage yields information on the kinetics of the transporter (Turner & Silverman, 1980). When the inhibitor I is added to the extracellular medium, it may bind both to the free and to the sodium-bound form of the transporter:

$$C'' + I \underset{q^*}{\overset{p^*}{\rightleftarrows}} C''I \tag{25}$$

$$MC'' + I \underset{q_M^*}{\overset{p_M^*}{\rightleftarrows}} MC''I. \tag{26}$$

The rate constants p^*, q^*, p_M^* and q_M^* are analogous to the rate constants p'', q'', p_M'', q_M'' of Fig. 1. Furthermore, the reaction

$$C''I + M^+ \underset{h_I}{\overset{g_I}{\rightleftarrows}} MC''I \tag{27}$$

has to be considered. Denoting the total fraction of transporter with bound inhibitor by x_I ($x_I \equiv x[C''I] + x[MC''I]$), the overall rate-constants k_{on} and k_{off} of binding and release of I are defined by

$$\left(\frac{dx_I}{dt}\right)_{t=0,x_I=0} = k_{on} c_I \tag{28}$$

$$\left(\frac{dx_I}{dt}\right)_{t=0,c_I=0} = -k_{off} x_I. \tag{29}$$

Equation (28) refers to an experiment in which at time $t = 0$ the inhibitor concentration is raised from zero to c_I, and Eq. (29) to an experiment in which the inhibitor concentration is reduced to zero at $t = 0$. Since k_{on} and k_{off} for phlorizin binding are small ($k_{on} c_I \simeq k_{off} \simeq 0.5$ sec^{-1} at $c_I = 3$ μM; *see* Toggenburger et al., 1982), it is likely to assume that in a phlorizin-binding (or release) experiment the other reactions (binding and release of Na^+, translocation of the free binding site) remain close to equilibrium. Under this condition k_{on} and k_{off} are given by (for $c'_S = c''_S = 0$):

$$k_{on} = \frac{p^* + p_M^* c''_M / K''_M}{1 + (c''_M / K''_M) + (1 + c'_M / K'_M) k''/k'} \tag{30}$$

$$k_{off} = \frac{q^* + q_M^* c''_M / K_M^I}{1 + c''_M / K_M^I}. \tag{31}$$

where $K'_M = h'/g'$, $K''_M = h''/g''$ and $K^I_M = h_I/g_I$. It is reasonable to assume that the rate constants p^*, p^*_M, q^* and q^*_M are only weakly voltage-dependent. A voltage effect on k_{on} and k_{off} may occur via the equilibrium constants K'_M, K''_M and K^I_M when sodium binding is voltage dependent. In this case both k_{on} and k_{off} are functions of voltage. If, however, the total voltage dependence of transport rate results from the transition $C' \rightleftarrows C''$ (rate constants k' and k''), only k_{on} will be affected by voltage.

Comparison with Experimental Results

Voltage effects on the rate of ion-driven cotransport have been demonstrated in experiments with renal or intestinal brush-border vesicles. It was found that an inside-negative membrane potential enhances Na^+-driven influx of D-glucose (Murer & Hopfer, 1974; Beck & Sacktor, 1975, 1978; Hilden & Sacktor, 1982; Kessler & Semenza, 1983; Kaunitz & Wright, 1984). Similar results were obtained with other cotransport systems, e.g., Na^+-coupled amino-acid transport in brush-border vesicles (Burckhardt, Kinne, Stange & Murer, 1980; Ganapathy & Leibach, 1983), Na^+-coupled sugar transport in epithelial cells (Carter-Su & Kimmich, 1980; Restrepo & Kimmich, 1985*a*) and H^+-coupled galactoside transport in *Escherichia coli* (Garcia, Viitanen, Foster & Kaback, 1983).

As mentioned above, information on the nature of voltage-dependent steps in Na^+-coupled D-glucose transport can be obtained from experiments with the competitive inhibitor phlorizin (Aronson, 1978; Turner & Silverman, 1981; Toggenburger et al., 1982; Restrepo & Kimmich, 1986). Inside-negative membrane potentials are found to increase the rate of phlorizin binding from the outside, whereas the dissociation rate is not affected by voltage. This observation has been interpreted by the assumption that the free binding site is negatively charged; under this condition an inside-negative potential decreases the ratio k''/k' in Eq. (30), corresponding to an increase of the fraction of transporter molecules with outward-facing binding sites (Toggenburger et al., 1982).

Quantitative studies of Na^+-driven sugar transport as a function of transmembrane voltage have been described by Kaunitz and Wright (1984) and by Restrepo and Kimmich (1985*a*). In both studies the sugar influx $-\Phi_S$ was found to be exponentially related to membrane potential according to $\Phi_S = \Phi_S^0 \exp(-\alpha u)$ within the experimental potential range, with α varying between ≈ 0 and 0.67, depending on the sugar concentration. It is clear from the foregoing discussion that a purely exponential flux-voltage behavior is possible under special conditions over an extended voltage range. For a 1 Na^+ : 1 S stoichiometry the flux-voltage relationship becomes exponential when the conformational transitions $C' \rightleftarrows C''$ and $MC'S \rightleftarrows MC''S$ are rate limiting and strongly voltage dependent ($\delta = 1$ in Eqs. (11) and (12)) and when the conditions $z_L = 0$, $\eta \approx -\frac{1}{2}$, or $z_L = -1$, $\eta \approx \frac{1}{2}$ are fulfilled. For a stoichiometry of 2 Na^+ : 1 S exponential behavior is predicted for $z_L = -1$, $\eta \approx 0$. In most cases, however, the flux saturates at large values of $|V|$ so that an (approximately) exponential flux-voltage relationship can be expected only in a limited voltage range (Figs. 4, 6 and 7). Experiments of the kind described by Kaunitz and Wright are likely to yield detailed insight into the mechanism of charge translocation by the cotransporter, as soon as more information on the nature of the rate-limiting steps of the transport process will become available.

The electrogenic effect of ion-driven cotransport systems may be studied directly by recording changes of membrane voltage or current after addition of substrate to the extracellular medium (Iwatsuki & Petersen, 1980; Frömter, 1982; Bergman & Bergman, 1985; *see* Gunter-Smith, Grasset & Schultz, 1982, for references to the earlier literature). In most of these studies conventional glass microelectrodes have been used, but more recently the technique of whole-cell recordings using patch-clamp micropipettes has been applied which allows internal perfusion of the cell (Jauch et al., 1986). By measuring the current-voltage characteristic of the cell membrane in the presence and in the absence of substrate, information on the current-voltage behavior of the cotransport system may be obtained.

Discussion

In this study a microscopic model for the analysis of voltage effects on ion-driven cotransport has been described. The model accounts for movements of ions and charged ligand groups as well as for reorientations of polar residues resulting from conformational transitions of the transport protein. The voltage dependence of the rate constants is given by a set of coefficients (β', β'', . . .) which reflect the dielectric distances over which charge is displaced in the elementary reaction steps. The dielectric coefficients are basic parameters for the description of any electrogenic transport system. They may be evaluated from the shape of the experimental flux-voltage (or current-voltage) curves, provided that sufficient information on the rate constants of the reaction cycle is available.

Even without explicit knowledge of the rate

constants of the transport system, a number of general predictions on the voltage dependence of fluxes are possible. A transport cycle of the type shown in Fig. 1 is likely to contain one or more voltage-independent or only weakly voltage-dependent reaction steps which at large voltages V become rate limiting. This means that, in general, the flux saturates for $|V| \to \infty$. Examples of saturation behavior are shown in Figs. 4, 6 and 7.

Another general prediction is that the flux-voltage characteristic may contain regions with negative slope where the flux decreases with increasing electrical driving force. This occurs when in one of the conformational transitions electric charges in the protein are displaced against the direction of overall charge movement. A current-voltage characteristic with a negative slope at inside-positive voltages has recently been observed in the case of the Na,K-pump (Lafaire & Schwarz, 1985).

An important parameter of the transport model is the voltage dependence of ion binding. The rate constants of ion-binding and -release are affected by voltage when part of the transmembrane field drops between binding site and external solution. Depending on the location of the binding site in conformations C' and C'' of the transporter, binding from the cytoplasm and from the extracellular medium may be affected by voltage to a different extent. In order to obtain information on the location of the binding site it is advantageous to study the flux-voltage relationship under asymmetric conditions, i.e., with zero ion concentration on one side and finite ion concentration on the other. Such experiments that require control of the cytoplasmic ion-concentration now become possible using the technique of whole-cell recording with patch-clamp pipettes (Marty & Neher, 1983; Jauch et al., 1986).

This work has been financially supported by Deutsche Forschungsgemeinschaft (Sonderforschungsbereich 156).

References

Aronson, P.S. 1978. Energy-dependence of phlorizin binding to isolated renal microvillus membranes. Evidence concerning the mechanism of coupling between the electrochemical Na^+ gradient and sugar transport. *J. Membrane Biol.* **42:**81–98

Aronson, P.S. 1984. Electrochemical driving forces for secondary active transport: Energetics and kinetics of Na^+-H^+ exchange and Na^+-glucose cotransport. *In:* Electrogenic Transport: Fundamental Principles and Physiological Implications. M.P. Blaustein and M. Liberman, editors. Raven, New York

Beck, J.C., Sacktor, B. 1975. Energetics of the Na^+-dependent transport of D-glucose in renal brush border membrane vesicles. *J. Biol. Chem.* **250:**8674–8680

Beck, J.C., Sacktor, B. 1978. The sodium electrochemical potential-mediated uphill transport of D-glucose in renal brush border membrane vesicles. *J. Biol. Chem.* **253:**5531–5535

Bergman, C., Bergman, J. 1985. Origin and voltage dependence of asparagine-induced depolarization in intestinal cells of *Xenopus* embryo. *J. Physiol. (London)* **366:**197–220

Burckhardt, G., Kinne, R., Stange, G., Murer, H. 1980. The effects of potassium and membrane potential on sodium-dependent glutamic acid uptake. *Biochim. Biophys. Acta* **599:**191–201

Carter-Su, C., Kimmich, G.A. 1980. Effects of membrane potential on Na-dependent sugar transport by ATP-depleted intestinal cells. *Am. J. Physiol.* **238:***C*73–*C*80

Crane, R.K., Dorando, F.C. 1982. The kinetics and mechanism of Na^+-gradient-coupled glucose transport. *In:* Membranes and Transport. A.N. Martonosi, editor. Vol. 2, pp. 153–160. Plenum, New York

Frömter, E. 1982. Electrophysiological analysis of rat renal sugar and amino acid transport. I. Basic phenomena. *Pfluegers Arch.* **393:**179–189

Ganapathy, V., Leibach, F.H. 1983. Electrogenic transport of 5-oxoproline in rabbit renal brush-border membrane vesicles. Effect of intravesicular potassium. *Biochim. Biophys. Acta* **732:**32–40

Garcia, M.L., Viitanen, P., Foster, D.L., Kaback, H.R. 1983. Mechanism of lactose translocation in proteoliposomes reconstituted with lac carrier protein purified from *Escherichia coli*. I. Effect of pH and imposed membrane potential on efflux, exchange, and counterflow. *Biochemistry* **22:**2524–2531

Geck, P., Heinz, E. 1976. Coupling in secondary transport. Effect of electrical potentials on the kinetics of ion-linked cotransport. *Biochim. Biophys. Acta* **443:**49–63

Gunter-Smith, P.J., Grasset, E., Schultz, S.G. 1982. Sodium-coupled amino acid and sugar transport by *Necturus* small intestine. *J. Membrane Biol.* **66:**25–39

Harrison, D.A., Rowe, G.W., Lumsden, C.F., Silverman, M. 1984. Computational analysis of models for cotransport. *Biochim. Biophys. Acta* **774:**1–10

Hilden, H., Sacktor, B. 1982. Potential-dependent D-glucose uptake by renal brush border membrane vesicles in the absence of sodium. *Am. J. Physiol.* **242:***F*340–*F*345

Hol, W.G.J. 1985. The role of the α-helix dipole in protein function and structure. *Prog. Biophys. Mol. Biol.* **45:**149–195

Hopfer, U., Groseclose, R. 1980. The mechanism of Na^+-dependent D-glucose transport. *J. Biol. Chem.* **255:**4453–4462

Iwatsuki, N., Petersen, O.H. 1980. Amino acids evoke short-latency membrane conductance increase in pancreatic acinar cells. *Nature (London)* **283:**492–494

Jardetzky, O. 1966. Simple allosteric models for membrane pumps. *Nature (London)* **211:**969–970

Jauch, P., Maruyama, Y., Petersen, O.H., Kolb, H.A., Läuger, P. 1986. Electrophysiological study of the alanine-sodium cotransporter in pancreatic acinar cells. *In:* 25 Years of Research on the Brush Border Membrane and on Sodium-Coupled Transport. INSERM Symposium Series Vol. 26. F. Alvarado and C.H. van Os, editors. Elsevier, Amsterdam *(in press)*

Johnson, K.J. 1980. Numerical Methods in Chemistry. Marcel Dekker, New York

Johnstone, R.M. 1979. Electrogenic amino acid transport. *Can. J. Physiol. Pharmacol.* **57:**1–15

Jung, D.W., Schwarz, W., Passow, H. 1984. Sodium-alanine cotransport in oocytes of *Xenopus laevis*. *J. Membrane Biol.* **78:**29–34

Kaback, H.R. 1983. The lac carrier protein in *Escherichia coli*. *J. Membrane Biol.* **76**:95–112

Kaunitz, H.D., Wright, E.M. 1984. Kinetics of sodium D-glucose cotransport in bovine intestinal brush border vesicles. *J. Membrane Biol.* **79**:41–51

Kessler, M., Semenza, G. 1983. The small-intestinal Na^+, D-glucose cotransporter: An asymmetric gated channel (or pore) responsive to $\Delta\psi$. *J. Membrane Biol.* **76**:27–56

Klingenberg, M., Riccio, P., Aquila, H., Buchanau, B.B., Grebe, K. 1976. *In:* The Structural Basis of Membrane Function. Y. Hatefi and L. Djavadi-Ohaniance, editors. pp. 293–311. Academic, New York

Lafaire, A.V., Schwarz, W. 1985. Voltage-dependent ouabain-sensitive current in the membrane of oocytes of *Xenopus laevis*. *In:* The Sodium Pump. I.M. Glynn and J.C. Ellory, editors. pp. 523–525. Company of Biologists, Cambridge, Great Britain

Läuger, P. 1980. Kinetic properties of ion carriers and channels. *J. Membrane Biol.* **57**:163–178

Läuger, P. 1984. Thermodynamic and kinetic properties of electrogenic ion pumps. *Biochim. Biophys. Acta* **779**:307–341

Marty, A., Neher, E. 1983. Tight-seal whole-cell recording. *In:* Single-channel recording. B. Sakmann and E. Neher, editors. pp. 107–122. Plenum, New York

Mitchell, P. 1969. Chemiosmotic coupling and energy transduction. *Theor. Exp. Biophys.* **2**:159–216

Murer, H., Hopfer, U. 1974. Demonstration of electrogenic Na^+-dependent D-glucose transport in intestinal brush border membranes. *Proc. Natl. Acad. Sci. USA* **71**:484–488

Overath, P., Wright, J.K. 1983. Lactose permease: A carrier on the move. *Trends Biochem. Sci.* **8**:404–408

Patlak, C.S. 1957. Contributions to the theory of active transport: II. The gate type noncarrier mechanism and generalizations concerning tracer flow, efficiency and measurements of energy expenditure. *Bull. Math. Biophys.* **19**:209–235

Restrepo, D., Kimmich, G.A. 1985*a*. The mechanistic nature of the membrane potential dependence of sodium-sugar cotransport in small intestine. *J. Membrane Biol.* **87**:159–172

Restrepo, D., Kimmich, G.A. 1985*b*. Kinetic analysis of the mechanism of intestinal Na^+-dependent sugar transport. *Am. J. Physiol.* **248**:*C*498–*C*509

Restrepo, D., Kimmich, G.A. 1986. Phlorizin binding to isolated enterocytes: Membrane potential and sodium dependence. *J. Membrane Biol.* **89**:269–280

Sanders, D., Hansen, U.-P., Gradmann, D., Slayman, C.L. 1984. Generalized kinetic analysis of ion-driven cotransport systems: A unified interpretation of selective ionic effects on Michaelis parameters. *J. Membrane Biol.* **77**:123–152

Schultz, S.G., Curran, P.F. 1970. Coupled transport of sodium and organic solutes. *Physiol. Rev.* **50**:637–718

Semenza, G., Kessler, M., Hosang, M., Weber, J., Schmidt, U. 1984. Biochemistry of the Na^+, D-glucose cotransporter of the small-intestinal brush-border membrane: The state of the art in 1984. *Biochim. Biophys. Acta* **779**:343–379

Stevens, B.R., Kaunitz, J.D., Wright, E.M. 1984. Intestinal transport of amino acids and sugars: Advances using membrane vesicles. *Annu. Rev. Physiol.* **46**:417–433

Toggenburger, G., Kessler, M., Semenza, G. 1982. Phlorizin as a probe for the small intestinal Na^+, D-glucose cotransporter. A model. *Biochim. Biophys. Acta* **688**:557–571

Turner, R.J. 1981. Kinetic analysis of a family of cotransport systems. *Biochim. Biophys. Acta* **649**:269–280

Turner, R.J. 1983. Quantitative studies of cotransport systems: Models and vesicles. *J. Membrane Biol.* **76**:1–15

Turner, R.J., Silverman, M. 1980. Testing carrier models of cotransport using the binding kinetics of non-transported competitive inhibitors. *Biochim. Biophys. Acta* **596**:272–291

Turner, R.J., Silverman, M. 1981. Interaction of phlorizin and sodium with the renal brush-border membrane D-glucose transporter: Stoichiometry and order of binding. *J. Membrane Biol.* **58**:43–55

Zwolinski, B.I., Eyring, H., Reese, C.E. 1949. Diffusion and membrane permeability. *J. Phys. Chem.* **53**:1426–1453

Received 27 January 1986; revised 14 March 1986